ACS APPLIED MATERIALS & INTERFACES
Letter
www.acsami.org

# Transformation of the Electrical Characteristics of Graphene Field-Effect Transistors with Fluoropolymer

Tae-Jun Ha,[†] Jongho Lee,[†] Sk. Fahad Chowdhury,[†] Deji Akinwande,[†] Peter J. Rossky,[‡] and Ananth Dodabalapur*[,†]

[†]Microelectronics Research Center and [‡]Department of Chemistry and Biochemistry, The University of Texas at Austin, Austin, Texas 78758, United States

*Supporting Information*

**ABSTRACT:** We report on the improvement of the electronic characteristics of monolayer graphene field-effect transistors (FETs) by an interacting capping layer of a suitable fluoropolymer. Capping of monolayer graphene FETs with CYTOP improved the on−off current ratio from 5 to 10 as well as increased the field-effect mobility by as much as a factor of 2 compared to plain graphene FETs. Favorable shifts in the Dirac voltage toward zero with shift magnitudes in excess of 60 V are observed. The residual carrier concentration is reduced to $\sim 2.8 \times 10^{11}$ cm$^{-2}$. Removal of the fluoropolymer from graphene FETs results in a return to the initial electronic properties before depositing CYTOP. This suggests that weak, reversible electronic perturbation of graphene by the fluoropolymer favorably tune the electrical characteristics of graphene, and we hypothesize that the origin of this improvement is in the strongly polar nature of the C−F chemical bonds that self-organize upon heat treatment. We demonstrate a general method to favorably restore or transform the electrical characteristics of graphene FETs, which will open up new applications.

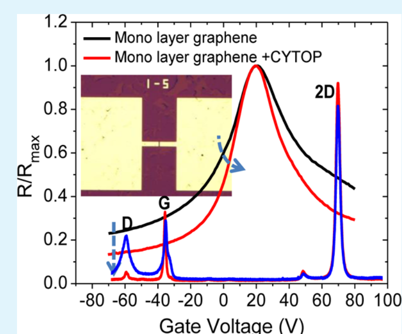


**KEYWORDS:** *graphene field-effect transistors, fluoropolymer, weak, reversible interactions, transformation of electrical characteristics, on−off current ratio, C−F bonds, functionalization*

## INTRODUCTION

Graphene is a very promising electronic material because of its high carrier mobility and stable mechanical and chemical properties.[1−6] Graphene-based field-effect transistors (FETs) have been shown to operate at very high frequencies.[7−9] Graphene FETs have a high off-current arising from residual carriers as well as the zero-bandgap.[10,11] In achieving such a transformation, the high mobility must not be reduced and preferably increased. In this letter, we demonstrate a general method to favorably transform the electrical characteristics of graphene FETs by capping with fluoropolymers such as CYTOP and Teflon-AF. The conductivity at the Dirac point is reduced and the mobility is increased, leading to an improvement in the on−off current ratio to ∼10. Remarkably, the key graphene device metrics are improved including electron−hole transport symmetry, Dirac voltage, and reduced impurity doping. We would like to point out that the effect described is not associated with graphene doping, but it is apparently a combination of phenomena resulting from ordered polar groups that form when fluoropolymer films are deposited on graphene. We present a hypothesis as to why this alteration happens. We note that, in general, attempts to coat graphene with inorganic dielectrics such as silicon dioxide and aluminum oxide have not resulted in an improvement in electrical characteristics. Importantly, these results have been achieved in graphene grown by wafer-scale chemical vapor deposition (CVD) process. From a practical standpoint, this is a significant advance in that it offers a clear path to improve the performance characteristics of graphene FETs in which the active material is grown by wafer-scale CVD. CVD graphene is the most promising method of realizing large area graphene and in adapting graphene for silicon CMOS and flexible electronics.[12] The improved mobilities and reduced conductivities will open up the range of applications for graphene circuitry.

## EXPERIMENTAL SECTION

Figure 1a shows the schematic cross-section of a monolayer graphene FET after capping with the fluoropolymer, CYTOP. As a first step, good-quality monolayer graphene films were synthesized on 500 nm thick e-beam evaporated copper films grown on silicon/silicon dioxide ($Si/SiO_2$) substrates, by the low-pressure chemical vapor deposition (LPCVD) as previously described.[13,14] In brief, the copper-coated Si/$SiO_2$ substrates were first annealed for 5 min at 1000 °C in hydrogen-saturated ambient. The hydrogen gas was purged away at the end of the annealing process and ultrahigh purity (99.99%) methane was circulated at a flow rate of 10 sccm for 5 min during the growth process. This results in the formation of a monolayer graphene on copper. After growth, the chamber was slowly cooled to below 180 °C before unloading of samples. Graphene on copper films were spin-

Received: October 31, 2012
Accepted: December 19, 2012
Published: December 19, 2012

 © 2012 American Chemical Society 

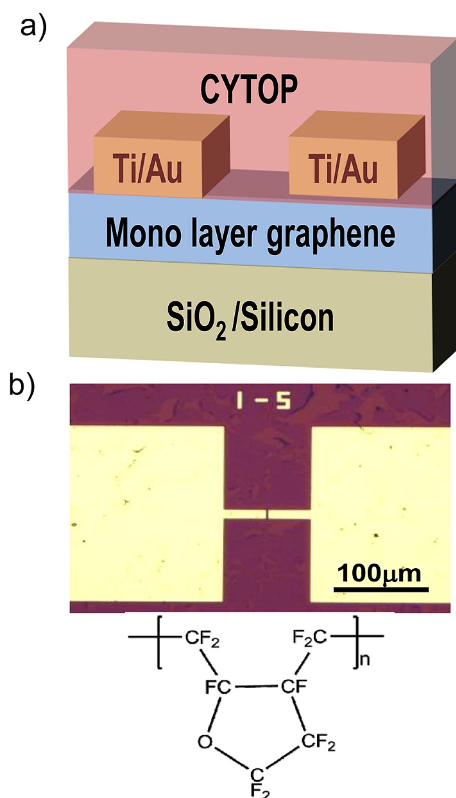


**Figure 1.** (a) Schematic cross-section and (b) optical image of a completed device and the chemical structure of CYTOP.

coated with poly(methyl methacrylate) (PMMA) at 4000 rpm for 1 min.

The graphene films were then transferred to the second Si/$SiO_2$ substrate by a conventional wet-transfer process.[13,14] In the wet-transfer process, the PMMA/graphene/copper layer was detached from the underlying Si/$SiO_2$ by etching away the sacrificial oxide in buffered oxide etch (6:1). Following this, the copper layer below graphene was etched in dilute ammonium persulfate solution to leave a free-standing film of graphene coated with PMMA. This free-standing film is transferred to a water bath where it is made to adhere to a fresh Si/$SiO_2$ substrate. This substrate possesses a 285 nm thick $SiO_2$ layer that subsequently functions as the gate insulator in FET devices. The PMMA is then removed with acetone.

Oxygen plasma reactive-ion-etching (RIE) was used to pattern the active channel region, to remove the superfluous graphene and to ensure device isolation. Source/drain electrodes were patterned by electron-beam lithography and lift-off. The titanium/gold (2.0 nm/50 nm) bilayers that form the source/drain contacts were deposited by thermal evaporation under high vacuum. Deposition of good quality titanium and gold in high vacuum conditions ($\sim 1 \times 10^{-7}$ Torr) are key to realizing low-resistance electrical contacts. The samples were kept in high vacuum for 2 days to minimize impurity incorporation. Monolayer graphene FETs fabricated as described above feature possess a channel width of 5 $\mu$m and a channel length of 1 $\mu$m, as shown in Figure 1b. After completing the entire fabrication of graphene FETs, Raman spectra were measured. The full width at half-maximum (fwhm) of the 2D peak is ~29 $cm^{-1}$.[15,16] The intensity ratio between 2D and G peaks is 2.8. The D peak intensity is small or negligible. These results indicate that the monolayer graphene in the FET is of high material quality.[13,14]

A 90 nm thick layer of the fluoropolymer, CYTOP (Asahi Glass Co.) was deposited by spin-coating a diluted CYTOP solution (CYTOP: CYTOP solvent = 1: 10) on monolayer graphene and annealed gradually from 30 to 180 °C for over a span of 1 h in a nitrogen atmosphere. A 140 nm thick layer of Teflon-AF (Dupont co.) was also spin-coated with as-supplied Teflon-AF solution on monolayer graphene. The samples were annealed gradually from 30 to 300 °C for over a span of 1 h in a nitrogen atmosphere. In order to remove the CYTOP from graphene FETs, the samples were immersed in a CYTOP solvent for 24 h. DC measurements for the device characteristics were carried out using an Agilent 4155C semiconductor parameter analyzer.

## RESULTS AND DISCUSSION

Figure 2a shows the transfer characteristics of as-deposited monolayer graphene FET without capping with CYTOP, with capping with CYTOP, and after removal of CYTOP. The drain-source voltage is 0.1 V during the sweep of the gate voltage from −70 to 80 V. It is generally observed that device characteristics such as on-state current, field-effect mobility and on−off current ratio in graphene FETs are reduced after the deposition of most dielectrics materials on graphene due to charge scattering (see the Supporting Information, Figure S1).[17−21] It is observed that in the present case, the off-state current (at the Dirac point) is decreased substantially, resulting in a net improvement in the on−off current ratio with the use of CYTOP. This is illustrated more clearly in Figure 2b, which shows that the on−off current ratio is improved from 5 to 10 after depositing CYTOP on graphene FETs. In addition, the field-effect mobility was improved from 1731 to 3606 $cm^2/(V\ s)$, width-normalized contact resistance is not appreciably altered from ~400 Ω $\mu$m and residual carrier density $n_o$ is reduced. The residual carrier density and the field-effect mobility are mainly determined from the minimum current at the Dirac point and the slope from the curves, respectively. The results indicate that electrical device characteristics of graphene FETs are significantly improved through the interaction

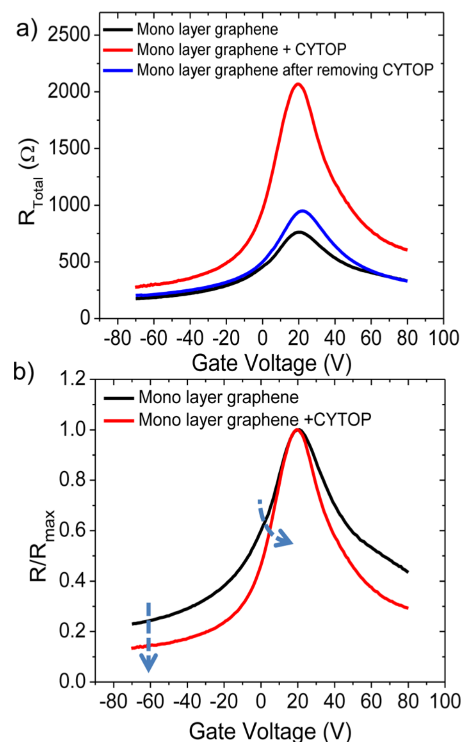


**Figure 2.** (a) Transfer characteristics of monolayer graphene, graphene with CYTOP capping layer, and graphene FETs after removing CYTOP .The drain-source voltage is 0.1 V. (b) Improvement in the normalized on−off current ratio after depositing CYTOP on monolayer graphene FET.

between fluoropolymer and monolayer graphene, which is different from the interaction of graphene with most dielectrics such as silicon dioxide, aluminum oxide and hafnium oxide.[17−21] When the CYTOP layer was removed by using CYTOP solvent from monolayer graphene FETs, the transfer characteristic tends to return to its initial state (i.e., that of monolayer graphene before CYTOP deposition), as shown in Figure 2a. There are spots where the CYTOP remains despite attempts to remove it. This results in the electrical characteristics reverting close to (but not exactly the same) as that of the graphene FETs before CYTOP application. The electronic properties of graphene can be tuned favorably using a capping layer of a material such as CYTOP and the interaction between graphene and CYTOP is weak enough to permit easy removal of CYTOP .[22,23]

Raman spectra were measured with a 442 nm blue laser on monolayer graphene capped with CYTOP. Figure 3 shows the

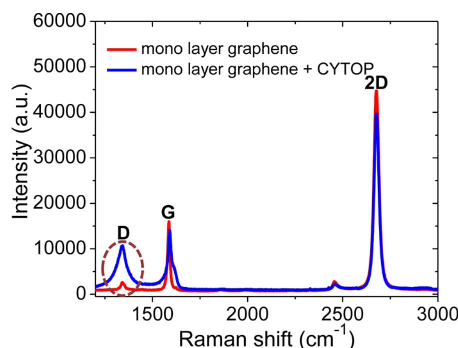


**Figure 3.** Change in Raman spectrum measured with a 442 nm blue laser of monolayer graphene with and without CYTOP capping layer.

change in the Raman spectrum of monolayer graphene produced by the capping layer of CYTOP. The intensity of the D band at 1350 $cm^{-1}$ was strongly increased after capping the graphene with CYTOP.[24] At the same time, the intensity of the 2D band at 2700 $cm^{-1}$ and the G band at 1580 $cm^{-1}$ were slightly decreased.[25,26] The C−F bonds in the CYTOP structure are very polar and graphene is a highly polarizable material.[27−29] The electronic interaction between the dipoles in the CYTOP and the graphene can modify its electronic properties significantly, leading to the effects that we observe. We note that with nonpolar organic capping layers such as pentacene, no significant changes in the electrical properties of graphene FETs are observed (see the Supporting Information, Figure S2). We have verified our hypothesis in the case of a second fluoropolymer, Teflon-AF possessing polar C−F bonds, which also results in a marked improvement in electrical properties of graphene upon capping. The origin of this improvement is in the strongly polar nature of the C−F chemical bond found in the capping materials we have employed together with the tendency of these materials to self-organize upon heat treatment such that there is an oriented layer of dipolar C−F bonds at the interface with graphene. This dipole layer results in a reduction of the dimensionless fine structure constant ($\alpha$).[30] A reduction in fine structure constant improves the mobility, which is limited by long-range scattering by charged impurities while simultaneously, the minimum conductivity, determined by short-range scattering, decreases.[30] This results in an improved on−off ratio, which has so far been a problem for graphene FETs.

Temperature-dependent mobility and impurity studies also show that with capping, the impurity scattering limited mobility continues to increase with reducing temperature which is accompanied by a reduction in $n_0$ as shown in Figure 4. The

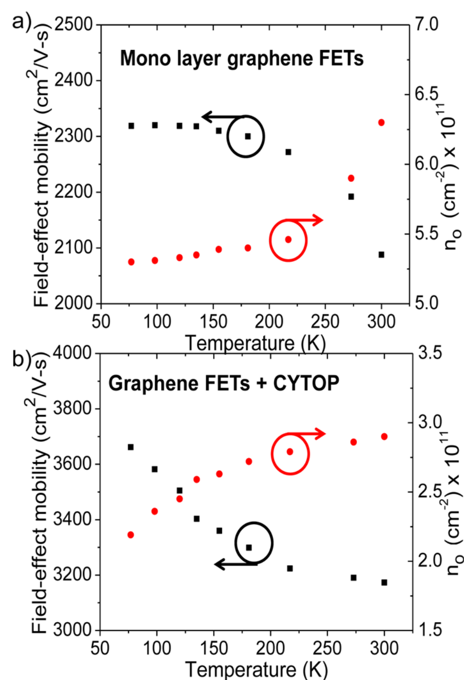


**Figure 4.** Temperature-dependent mobility and $n_o$ in (a) monolayer graphene FETs vs (b) graphene FETs capped with CYTOP: Studies show that with capping, the impurity scattering limited mobility continues to increase with reducing temperature, which is accompanied by a reduction in $n_o$.

residual carrier concentration is reduced to ∼$2.8 \times 10^{11}$ $cm^{-2}$ at room temperature when employing the capping layer of a fluoropolymer on graphene. The CYTOP dipoles could also break the symmetry between the A and B sublattices in graphene, leading to the development of a small energy gap, which is also consistent with our results.[31−34]

The effect of capping with fluoropolymer on highly doped monolayer graphene FETs is shown in Figure 5. Before coating, the graphene FETs possess a very positive Dirac voltage of 80 V and asymmetric electron and hole transport. Upon coating with

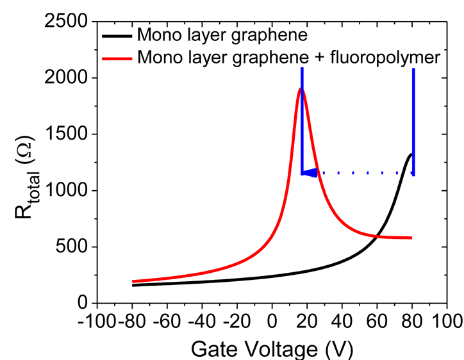


**Figure 5.** Transformation of characteristics of monolayer graphene by capping with Teflon-AF at a drain-source voltage of 0.1 V, with the gate bias swept from −80 V to 80 V; the substantial shift in the Dirac voltage toward zero after depositing Teflon-AF can be noted.

the Teflon-AF and annealing at 300 °C, we observe a remarkable shift in the Dirac voltage toward zero with shift magnitudes in excess of 60 V. In addition, electron and hole transport becomes more symmetric and the on−off current ratio improved from 6 to 8 as well as the field-effect mobility was increased from 1700 to 3452 $cm^2$/V-s without change in width-normalized contact resistance. In addition, the residual carrier density $n_o$ is reduced from $2.3 \times 10^{12}$ to $4.6 \times 10^{11}$ $cm^{-2}$. We also observed a shift in Dirac voltage of around 50 V toward zero for graphene FETs capped with CYTOP. The fluorocarbon capping method is therefore a way to restore or greatly improve the properties of graphene that are otherwise nonideal when formed using a combination of CVD and transfer methods.

It is meaningful that a significant favorable modification of electronic properties of monolayer graphene FETs can occur with the introduction of the selected organic material without a complicated fluorination fabrication process. A similar effect of capping layer of fluorinated semiconductor, hexadecafluoro-copperphthallocyanine ($F_{16}CuPc$) was observed on monolayer graphene FETs.[21] Compared to the plain graphene FET, capping with $F_{16}CuPc$ improved on−off current ratio from 3 to 5 as well as the field-effect mobility from 1292 to 1367 $cm^2$/(V s) (see the Supporting Information, Figure S3). High deposition temperatures will lead to a more crystalline, π-stacked phthalocyanine structure with the fluorinated periphery presenting to the graphene interface.

The capping materials that we have chosen all possess C−F bonds and processing conditions have been employed that results in the materials ordering in a manner that results in a strong net dipole moment at the interface with graphene. Additional experiment and theoretical work is being done to understand these effects in more detail and will be reported elsewhere. The fact that the strength of this interaction is dependent on the annealing temperature of the CYTOP and Teflon-AF also suggests that annealing improves the ordering of the fluoropolymer and consequently the total dipole strength. In the case of the two fluoropolymers postdeposition annealing (at temperatures up to 300 °C) was employed to enable material reorganization and the side chain alignment that is commonly observed in these materials. For the organic semiconductor, $F_{16}CuPc$, material deposition was performed at elevated temperatures (up to 200 °C). Previous work has shown that such elevated deposition temperatures results in the best ordered materials resulting in relatively high mobility in these semiconducting films.[35] It can be clearly observed (see the Supporting Information, Figure S4) that the electrical properties of CYTOP-coated graphene steadily improve with annealing temperature (in the range 60−180 °C) demonstrating that the side-chain alignment that accompanies such annealing is a key factor in the transformation of electrical properties. It is noteworthy that if the CYTOP is removed after the annealing, then the original graphene characteristics are recovered indicating reversible noncovalent interactions. While many of these results can be explained in terms of a modification of the fine structure constant, we note that graphene is very polarizable and changes to the electronic structure and, consequently transport properties, can result from having oriented dipoles topping the graphene. Additionally, we have modified the electronic environment on only one side of the graphene monolayer. If both interfaces have highly polar bonds juxtaposed, then the favorable effects we report can be further enhanced.

## CONCLUSION

In summary, we have shown that the electrical characteristics of graphene are favorably altered by capping with the fluoropolymer CYTOP and Teflon-AF. The on−off current ratio is improved and the Dirac voltage shifted toward zero. The residual carrier density $n_o$ is reduced and the mobility increased by as much as a factor of 2. We hypothesize that this alteration in electrical properties is a result of electronic polarization of the graphene by local C−F dipoles in the fluoropolymer. The strength of this interaction is dependent on the annealing temperature, which influences the ordering of the polymer and consequently the local dipole field. The approach we described offers a way to transform the electrical characteristics of graphene making it potentially more useful for a wider range of electronic applications.

## ASSOCIATED CONTENT

### Supporting Information

The transfer characteristics of monolayer graphene FETs with and without a capping layer of silicon dioxide; The total resistance of monolayer graphene with and without capping with Pentacene; Output characteristics of optimized bottom gate bottom contact $F_{16}CuPc$ FET and the total resistance in monolayer graphene and graphene FETs capped with $F_{16}CuPc$; The electrical properties of CYTOP-coated graphene FETs with annealing temperatures; Illustration of fabrication process flow of a monolayer graphene FET after capping with the fluoropolymer. This material is available free of charge via the Internet at http://pubs.acs.org.

## AUTHOR INFORMATION

**Corresponding Author**

*E-mail: ananth.dodabalapur@engr.utexas.edu.

**Notes**

The authors declare no competing financial interest.

## ACKNOWLEDGMENTS

This work is supported by NSF-ECCS under Grant 0901683 and an ONR Grant in the program of Dr. Chagaan Baatar. We also thank the NSF NERC "NASCENT" for support. P.J.R. thanks the NSF (CHE-0910499) and the R. A. Welch Foundation (F-0019) for support.

## REFERENCES

(1) Avouris, P. *Nano Lett.* **2010**, *10*, 4285.
(2) Bolotin, K. I.; Sikes, K. J.; Jiang, Z.; Klima, M.; Fudenberg, G.; Hone, J.; Kim, P.; Stormer, H. L. *Solid State Commun.* **2008**, *146*, 351.
(3) Stankovich, S.; Dikin, D. A.; Dommett, G. H. B.; Kohlhaas, K. M.; Zimney, E. J.; Stach, E. A.; Piner, R. D.; Nguyen, S. T.; Ruoff, R. S. *Nature* **2006**, *442*, 282.
(4) Booth, T. J.; Blake, P.; Nair, R. R.; Jiang, D.; Hill, E. W.; Bangert, U.; Bleloch, A.; Gass, M.; Novoselov, K. S.; Katsnelson, M. I.; Geim, A. K. *Nano Lett.* **2008**, *8*, 2442.
(5) Geim, A. K.; Novoselov, K. S. *Nat. Mater.* **2007**, *6*, 183.
(6) Kim, S.; Nah, J.; Jo, I.; Shahrjerdi, D.; Colombo, L.; Yao, Z.; Tutuc, E.; Banerjee, S. K. *Appl. Phys. Lett.* **2009**, *94*, 062107.
(7) Lin, Y.-M.; Dimitrakopoulos, C.; Jenkins, K. A.; Farmer, D. B.; Chiu, H.-Y.; Grill, A.; Avouris, P. *Science* **2010**, *327*, 662.
(8) Wu, Y.; Jenkins, K. A.; Valdes-Garcia, A.; Farmer, D. B.; Zhu, Y.; Bol, A. A.; Dimitrakopoulos, C.; Zhu, W.; Xia, F.; Avouris, P.; Lin, Y.-M. *Nano Lett.* **2012**, *12*, 3062.
(9) Wang, H.; Nezich, D.; Kong, J.; Palacios, T. *IEEE Electron Device Lett.* **2009**, *30*, 547.

(10) Xia, F.; Farmer, D. B.; Lin, Y.-M.; Avouris, P. *Nano Lett.* **2010**, *10*, 715.
(11) Schwierz, F. *Nat. Nanotechnol.* **2010**, *5*, 487.
(12) Li, X.; Cai, W.; An, J.; Kim, S.; Nah, J.; Yang, D.; Piner, R.; Velamakanni, A.; Jung, I.; Tutuc, E.; Banerjee, S. K.; Colombo, L.; Ruoff, R. S. *Science* **2009**, *324*, 1312.
(13) Tao, L.; Lee, J.; Chou, H.; Holt, M.; Ruoff, R. S.; Akinwande, D. *ACS Nano* **2012**, *6*, 2319.
(14) Lee, J.; Tao, L.; Hao, Y.; Ruoff, R. S.; Akinwande, D. *Appl. Phys. Lett.* **2012**, *100*, 152104.
(15) Ferrari, A. C.; Meyer, J. C.; Scardaci, V.; Casiraghi, C.; Lazzeri, M.; Mauri, F.; Piscanec, S.; Jiang, D.; Novoselov, K. S.; Roth, S.; Geim, A. K. *Phys. Rev. Lett.* **2006**, *97*, 187401.
(16) Graf, D.; Molitor, F.; Ensslin, K.; Stampfer, C.; Jungen, A.; Hierold, C.; Wirtz, L. *Nano Lett.* **2007**, *7*, 238.
(17) Lemme, M. C.; Echtermeyer, T. J.; Baus, M.; Szafranek, B. N.; Bolten, J.; Schmidt, M.; Wahlbrink, T.; Kurz, H. *Solid-State Electron.* **2008**, *52*, 514.
(18) Lin, Y.-M.; Chiu, H.-Y.; Jenkins, K. A.; Farmer, D. B.; Avouris, P.; Valdes-Garcia, A. *IEEE Electron Device Lett.* **2010**, *31*, 68.
(19) Chen, F.; Xia, J.; Ferry, D. K.; Tao, N. *Nano Lett.* **2009**, *9*, 2571.
(20) Fallahazad, B.; Kim, S.; Colombo, L.; Tutuc, E. *Appl. Phys. Lett.* **2010**, *97*, 123105.
(21) Ha, T.-J.; Akinwande, D.; Dodabalapur, A. *Appl. Phys. Lett.* **2012**, *101*, 033309.
(22) Lee, B.; Chen, Y.; Duerr, F.; Mastrogiovanni, D.; Garfunkel, E.; Andrei, E. Y.; Podzorov, V. *Nano Lett.* **2010**, *10*, 2427.
(23) Guo, B.; Liu, Q.; Chen, E.; Zhu, H.; Fang, L.; Gong, J. R. *Nano Lett.* **2010**, *10*, 4975.
(24) Lee, W. H.; Suk, J. W.; Chou, H.; Lee, J.; Hao, Y.; Wu, Y.; Piner, R.; Akinwande, D.; Kim, K. S.; Ruoff, R. S. *Nano Lett* **2012**, *12*, 2374.
(25) Robinson, J. T.; Burgess, J. S.; Junkermeier, C. E.; Badescu, S. C.; Reinecke, T. L.; Perkins, F. K.; Zalalutdniov, M. K.; Baldwin, J. W.; Culbertson, J. C.; Sheehan, P. E.; Snow, E. S. *Nano Lett.* **2010**, *10*, 3001.
(26) Nair, R. R.; Ren, W.; Jalil, R.; Riaz, I.; Kravets, V. G.; Britnell, L.; Blake, P.; Schedin, F.; Mayorov, A. S.; Yuan, S.; Katsnelson, M. I.; Cheng, H. −M.; Strupinski, W.; Bulusheva, L. G.; Okotrub, A. V.; Grigorieva, I. V.; Grigorenko, A. N; Novoselov, K. S.; Geim, A. K. *Small* **2010**, *6*, 2877.
(27) Graupe, M.; Takenaga, M.; Koini, T.; Colorado, R.; Lee, T. R. *J. Am. Chem. Soc.* **1999**, *121*, 3222.
(28) Sarma, S. D.; Adam, S.; Hwang, E. H.; Rossi, E. *Rev. Mod. Phys.* **2011**, *83*, 407.
(29) Duarte, D.; Dodabalapur, A. *J. Appl. Phys.* **2012**, *111*, 044509.
(30) Jang, C.; Adam, S.; Chen, J.-H.; Williams, E. D.; Das Sarma, S.; Fuhrer, M. S. *Phy. Rev. Lett.* **2008**, *101*, 146805.
(31) Dalvi, V. H.; Rossky, P. J. *Proc. Natl. Acad. Sci. U.S.A.* **2010**, *107*, 13603.
(32) Zhou, S. Y.; Gweon, G.-H.; Fedorov, A. V.; First, P. N.; de Heer, W. A.; Lee, D. −H.; Guiena, F.; Castro Neto, A. H.; Lanzara, A. *Nature Mat.* **2007**, *6*, 770.
(33) Vitali, L.; Riedl, C.; Ohmann, R.; Brihuega, I.; Starke, U.; Kern, K. *Surf. Sci.* **2008**, *602*, L127.
(34) Sahin, H.; Topsakal, M.; Ciraci, S. *Phys. Rev. B.* **2011**, *83*, 115432.
(35) Crone, B.; Dodabalapur, A.; Lin, Y.-Y.; Filas, R. W.; Bao, Z.; LaDuca, A.; Sarpeshkar, R.; Katz, H. E.; Li, W. *Nature* **2000**, *403*, 521.